Smart Cu(II)-aptamer complexes based gold nanoplatform for tumor micro-environment triggered programmable intracellular prodrug release, photodynamic treatment and aggregation induced photothermal therapy of hepatocellular carcinoma

Da Zhang[a,b], Aixian Zheng[a,b], Juan Li[d], Ming Wu[a,b], Lingjie Wu[a,b], Zuwu Wei[a,b], Naishun, Liao[a,b], Xiaolong Zhang[a,b], Zhixiong Cai[a,b], Huanghao Yang[d], Gang Liu[e], Xiaolong Liu[a,b]*, Jingfeng Liu[a,b,c]*

[a.] The United Innovation of Mengchao Hepatobiliary Technology Key Laboratory of Fujian Province, Mengchao Hepatobiliary Hospital of Fujian Medical University, Fuzhou 350025, P. R. China

[b.] The Liver Center of Fujian Province, Fujian Medical University, Fuzhou 350025, P. R. China

[c.] Liver Disease Center, The First Affliated Hospital of Fujian Medical University, Fuzhou 350005, P. R. China

[d.]The Key Lab of Analysis and Detection Technology for Food Safety of the MOE, Fujian Provincial Key Laboratory of Analysis and Detection Technology for Food Safety, College of Chemistry, Fuzhou University, Fuzhou 350002, P.R. China

[e.] Center for Molecular Imaging and Translational Medicine, Xiamen University, Xiamen, 361005, P. R. China

* Corresponding Author (correspondence should be address to Xiaolong Liu and Jingfeng Liu), E-mail addresses: xiaoloong.liu@gmail.com, drjingfeng@126.com

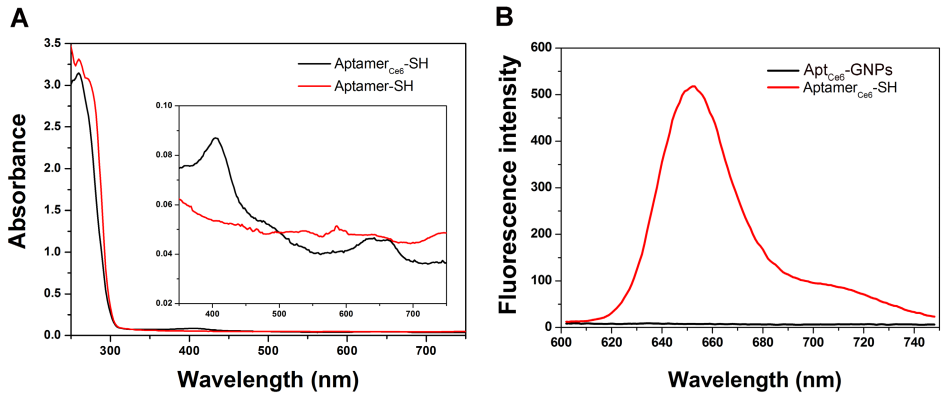

Figure S1, (A) The Vis-NIR spectra of Aptamer-SH and Aptamer$_{Ce6}$-SH; (B) The fluorescence spectra of Aptamer$_{Ce6}$ and Apt$_{Ce6}$-GNPs.

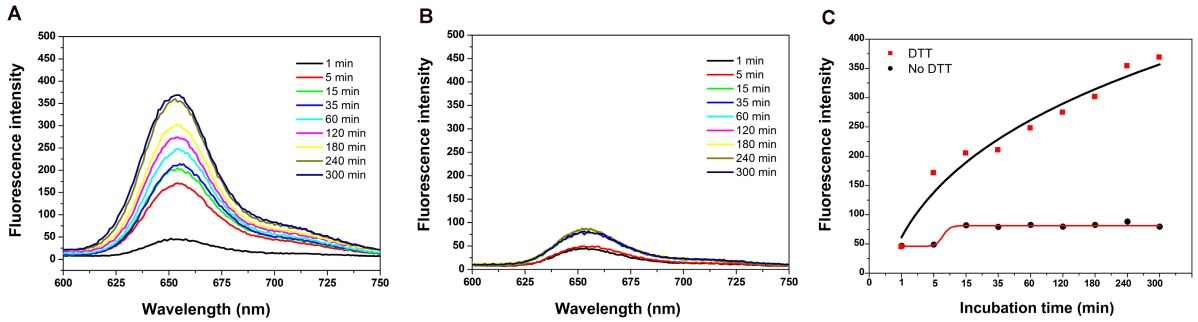

Figure S2, (A) The fluorescence spectra of Apt$_{Ce6}$-GNPs in the presence of DTT (10 mM) with different incubation times; (B) The fluorescence spectra of Apt$_{Ce6}$-GNPs in the absence of DTT (10 mM) with different incubation times; (C) Fluorescence recovery of Apt$_{Ce6}$-GNPs with or without DTT under different incubation times.

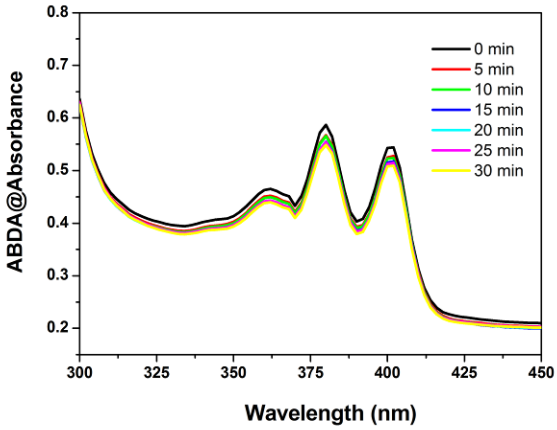

Figure S3, The absorbance of 9, 10-dimethylanthracene (ABDA, 100 μM) after photodecomposition by ROS generation upon 670 nm laser irradiation at 0.5 W/cm^2 in the presence of Apt$_{Ce6}$-GNPs but without incubated with DTT (10 mM) in PBS solution;

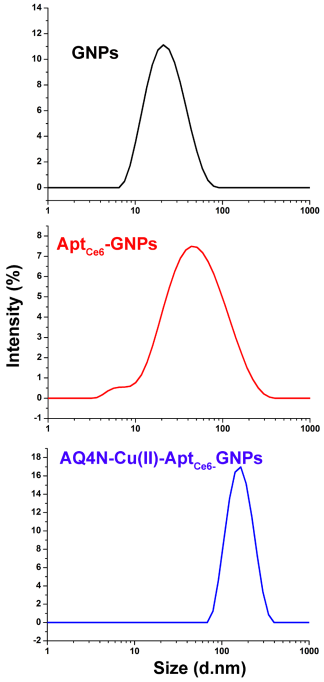

Figure S4, Hydrodynamic size distribution of GNPs, Apt$_{Ce6}$-GNPs and AQ4N-Cu(II)-Apt$_{Ce6}$-GNPs in water.

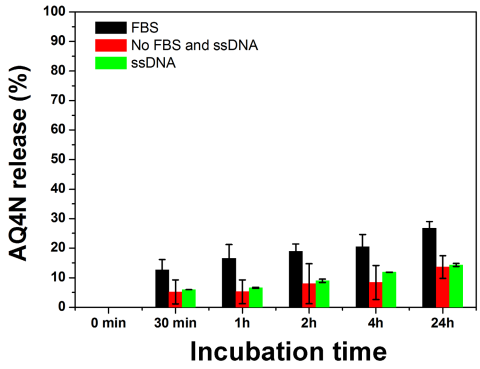

Figure S5, The cumulative AQ4N release kinetics of AQ4N-Cu(II)-Apt$_{Ce6}$-GNPs in PBS buffer (pH 7.4) supplemented with 10% FBS or 10 μM ssDNA at 37ºC (n=3).

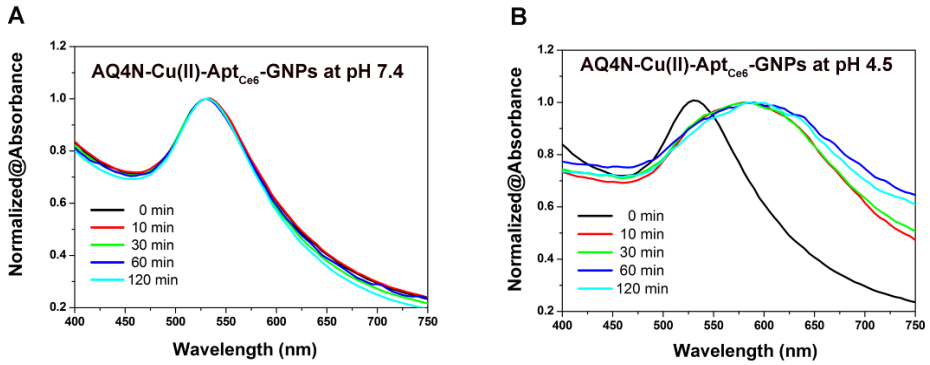

Figure S6, (A) Vis-NIR spectra of AQ4N-Cu(II)-Apt$_{Ce6}$-GNPs in pH 7.4. (B) Vis-NIR spectra of AQ4N-Cu(II)-Apt$_{Ce6}$-GNPs in pH 4.5.

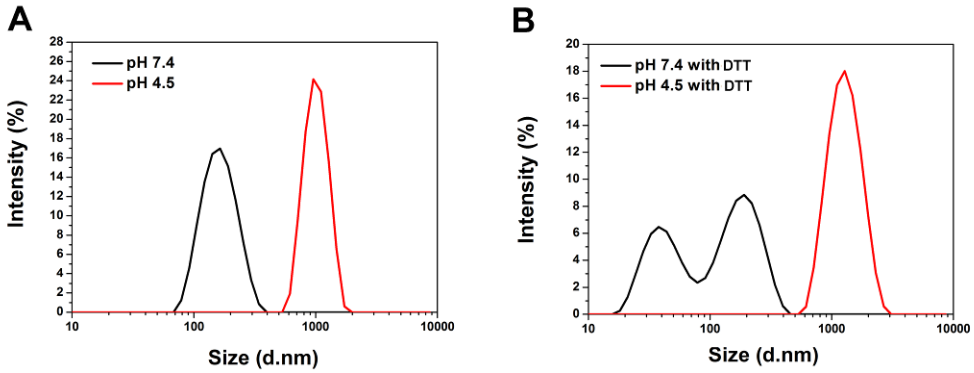

Figure S7, Hydrodynamic size distribution of AQ4N-Cu(II)-Apt$_{Ce6}$-GNPs under different pH conditions with (A) or without incubation with 10 mM DTT (B).

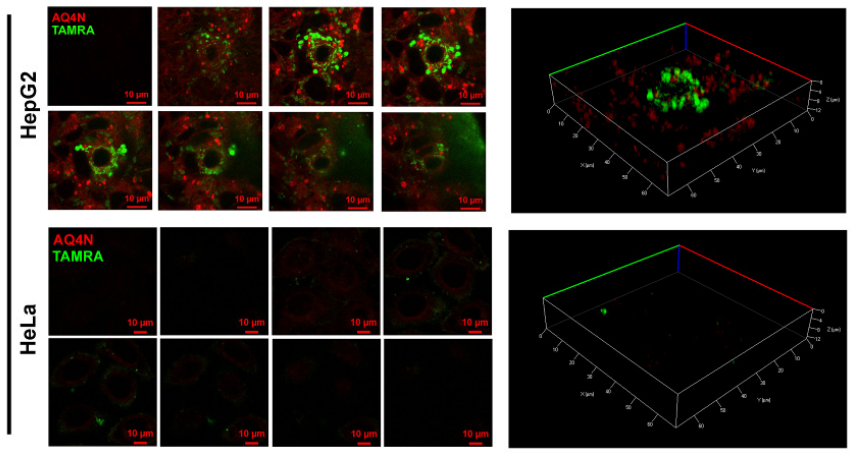

Figure S8, Confocal images of HepG2 cells or HeLa cells which were incubated with AQ4N-Cu(II)-Apt$_{TAMRA}$-GNPs for 4hrs.

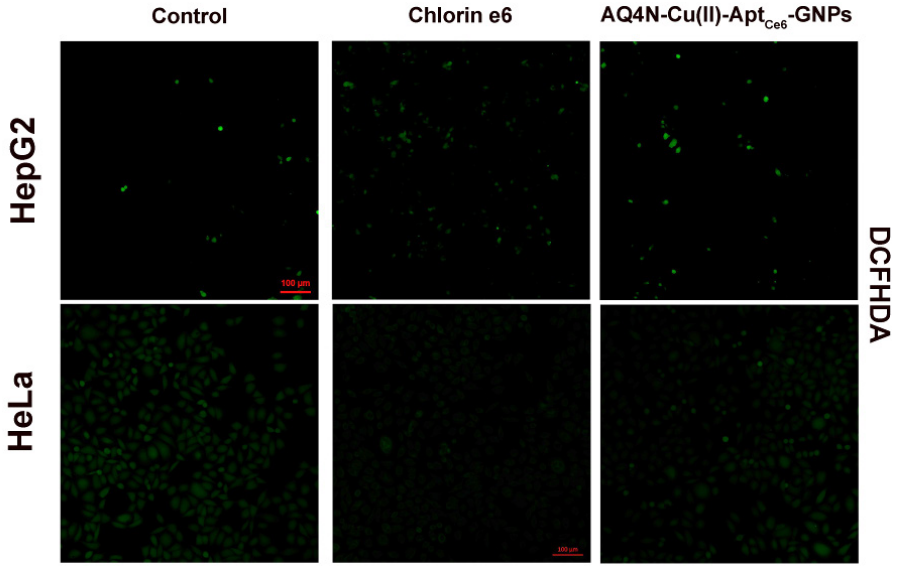

Figure S9, Confocal images of HepG2 cells and HeLa cells that received different treatments as indicated: the cells treated with free Ce6 or AQ4N-Cu(II)-Apt$_{Ce6}$-GNPs without laser irradiation, and none treated cells were taken as control; DCFH-DA was taken as the ROS indicator (scale bar = 50 μm).

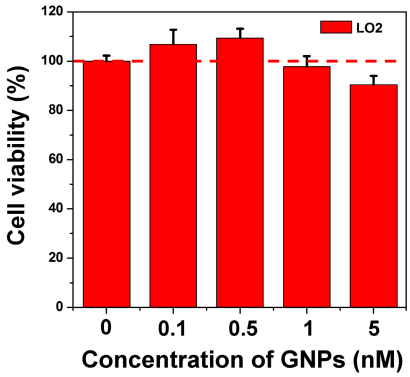

Figure S10, Cell viability of LO2 cells treated with different concerntration of AQ4N-Cu(II)-Apt$_{Ce6}$-GNPs (n = 6).

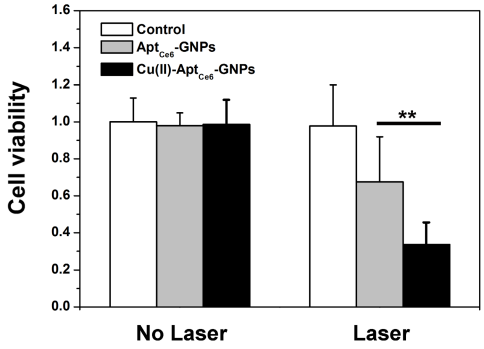

Figure S11, (C) Cell viability of HepG2 cells treated with Apt$_{Ce6}$-GNPs or Cu(II)-Apt$_{Ce6}$-GNPs with or without laser irradiation (670 nm, 0.5 W/cm^2) (n = 6), and the statistical analysis was performed with the two-tailed paired Student's T-test, **p<0.01.

.

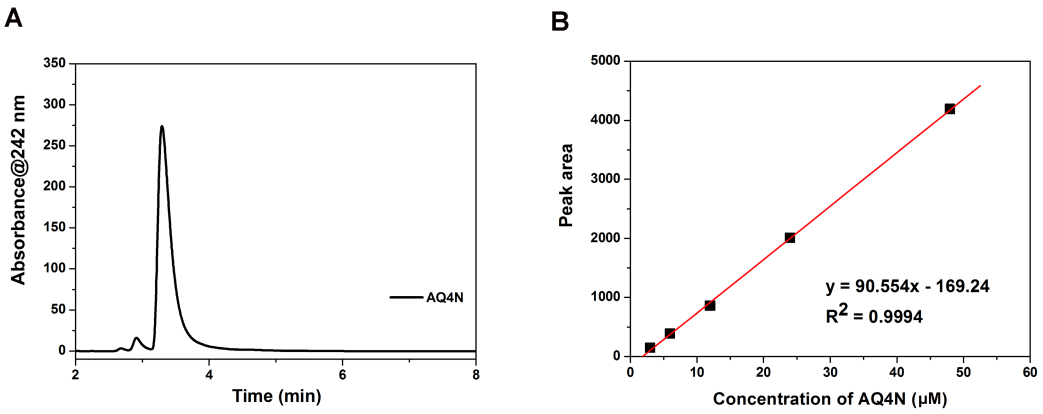

Figure S12, (A) Chromatograms of the AQ4N standard (48 μM); (B)The peak area of various concentration of AQ4N from 2 μM to 48 μM at the retention time of 3.297 min.

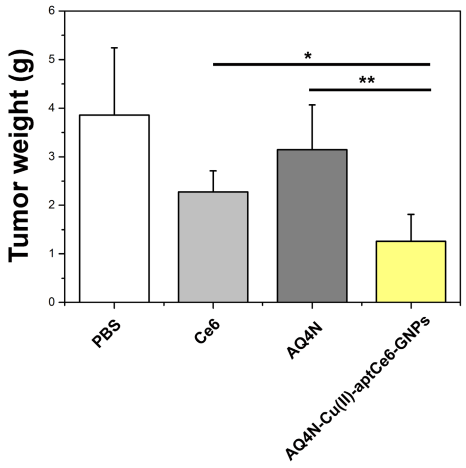

Figure S13, The average tumor weight of PBS, Ce6, AQ4N-Cu(II)-Apt$_{Ce6}$-GNPs treated mice when exposed to an 670 nm laser irradiation (0.5 W/cm^2) or AQ4N treated mice at the 18 days (n=4), and statistical analysis was performed with the two-tailed paired Student's T-test, *p<0.05, **p<0.01.

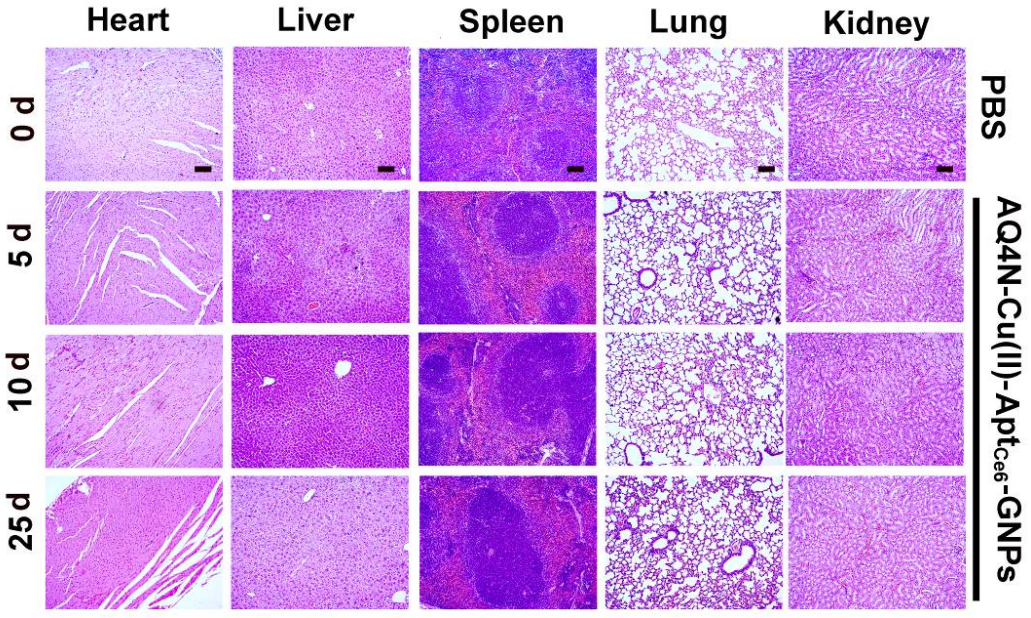

Figure S14. The pathological changes of main organs evaluated by H&E staining which were acquired at different time intervals post intravenous injection of AQ4N-Cu(II)-Apt$_{Ce6}$-GNPs. (Scale bar: 50 μm). No noticeable pathological changes were observed in these organs.